Anal Bioanal Chem (2007) 387: 791–801
DOI 10.1007/s00216-006-0684-y

ORIGINAL PAPER

Francesca Casadio · Janet G. Douglas · Katherine T. Faber

Noninvasive methods for the investigation of ancient Chinese jades: an integrated analytical approach

Received: 30 May 2006 / Revised: 5 July 2006 / Accepted: 14 July 2006 / Published online: 16 August 2006
© Springer-Verlag 2006

Abstract This paper reports on an integrated analytical approach for the noninvasive characterization of Chinese nephrite samples, encompassing both geological reference specimens and museum objects. Natural variations induced by cationic substitutions, as well as human-induced alterations such as heating, which both affect color, are the focus of this contribution. Totally noninvasive methods of analysis were used, including X-ray fluorescence spectroscopy, Raman microspectroscopy, visible reflectance spectroscopy and X-ray diffraction; moreover, the feasibility of using a portable Raman spectrometer for the in-field identification of jades has been demonstrated. Fe/Fe+Mg (% p.f.u.) ratios of the jades have been calculated based on hydroxyl stretching Raman bands, which will provide an important addition to similar data that are being collected at major museums in the Western and Eastern hemispheres.

Keywords Jade · Nephrite · XRD · Raman spectroscopy · Visible spectrophotometry

F. Casadio (✉)
Department of Conservation Science,
The Art Institute of Chicago,
111 S. Michigan Ave,
Chicago, IL 60603, USA
e-mail: fcasadio@artic.edu

J. G. Douglas
Department of Conservation and Scientific Research,
Freer Gallery of Art and Arthur M. Sackler Gallery,
Smithsonian Institution,
Washington, DC 20560, USA

K. T. Faber
Department of Materials Science and Engineering,
Northwestern University,
Evanston, IL 60208, USA

Introduction

In the early history of China, jade was highly regarded and used extensively for ritual objects, decoration, utilitarian objects such as tools, and burial goods. Quality and color (termed *Yu De* and *Yu Fu* in ancient Chinese) were the two fundamental parameters used to judge the "virtue" of jade [1]. Early jades from China are typically composed of nephrite, a massive, fine-grained variety of the tremolite–actinolite series of amphiboles ($Ca_2Mg_5Si_8O_{22}(OH)_2$ and $Ca_2MgFe_4Si_8O_{22}(OH)_2$, respectively) that consists of interlocking fibrous crystals, although other stone materials were used as well.

Research using scientific methods performed over the last decade has focused on the mineralogical identification of these materials, as well as the geological source of jade, early jade working methods, the detection of heating in jade, burial alteration, and surface accretions, using a wide range of analytical methods [2]. In particular, noninvasive techniques are finding support in studies of significant collections of Chinese jades dating from the Neolithic period (5000 to 1700 BCE) to the Han dynasty (206 BCE to 220 CE) at major art museums. These studies help the art historian to develop the cultural and archaeological contexts of jade objects. Studies of unearthed jades, in particular, are invaluable for determining the cultural context of jade of uncertain origin, which is the situation with most jades in Western collections [3–7].

Spectroscopic methods of analysis have been increasingly applied to the study of jades, most commonly for basic mineralogical identification [8, 9]. Other research has aimed at answering questions beyond the mineral content. New Zealand jade composed of nephrite has been investigated by a combination of infrared, optical absorption spectroscopy, Mössbauer spectroscopy and other chemical and petrologic methods in order to better understand the color of nephrite from that region [10]. Of particular interest is the use of noninvasive Raman microscopy (RM) in the study of Mesoamerican jadeite pebbles from Guatemala, where the mineral phases present in the jade were used to classify the rock type [11]. Data

from this study will continue to be useful for geologic sourcing studies when compared to compositional data of Pre-Columbian jade artifacts [12]. The application of RM to jadeite is well demonstrated, and could become a routine approach in archaeometry for identification and provenance studies, especially as inexpensive portable Raman microprobes are developed with improved spectral resolution (up to 8 cm^{-1}).

X-ray fluorescence spectroscopy (XRF) has been applied to the study of Chinese jades composed of nephrite in order to determine the minor elemental compositions of these objects, and hence, more about their geologic source in China [13, 14]. A combined, noninvasive, external beam particle-induced X-ray emission (PIXE) and RM study has been applied to six ancient Chinese jades [15]. This work, performed at the Guimet Asian Museum in Paris, was aimed at the determination of cation composition and distribution in nephrite, which served as a way to understand the color in jade and the provenance of ancient Chinese jades. Recently, approximately twenty ancient Chinese nephrite objects from the collection of the British Museum in London were studied with RM and scanning electron microscopy with elemental microanalysis (SEM/EDX) to address similar questions [16].

The current study builds on this research, and focuses specifically on the use of noninvasive methods that are ideally suited to the study of ancient Chinese jades, because the analysis can be done without risking damage to precious artifacts, and several areas on the surface of an object can be probed, thus allowing comprehensive mapping of the phases present. In addition to determinations of mineral content, the methods are useful for studying the chemical causes of color in nephrite, determining heating in jade, and further surface characterization. Additionally, the successful demonstration of the applicability of a portable micro-Raman spectrophotometer to the precise characterization of these materials will be valuable for the study and classification of excavated jades at archaeological sites in China. Together these techniques provide us with a powerful tool for characterizing jade materials used by people in ancient China, and for building a database that will allow the study of unprovenanced Chinese jades.

Experimental methods

The objects examined are described in Tables 1 and 2 and Figs. 1 and 2. They include modern nephrite reference specimens of known geological origin from China and neighboring regions (a possible source of jade in ancient times), as well as selected museum objects dated from the Neolithic (third millennium BCE) to the Shang dynasty (second millennium BCE). All of the objects were selected on the basis of color, ranging from translucent white to almost black.

To study the effect of heat treatment, a low-iron tremolitic nephrite pebble from Hetian (Khotan) in Xinjiang Province was cut with a diamond saw into different slices, each polished on one side and individually heated in a muffle furnace in oxidizing atmosphere for 24 hours at temperatures ranging from 500 °C to 1100 °C in increments of 100 °C, as already previously described in detail [17]. One unheated sample was kept as a control.

Table 1 Modern reference geological samples of nephrite from China and neighboring regions, arranged from lightest to darkest perceived color

Sample	Provenance	Description	Color (CIELab coordinates)	λ of major absorption vis spectrum (nm)	λ_{max} R% (nm)	Apparent composition (Raman) (Fe/Fe + Mg)(% p.f.u.)	Elemental composition detected by XRF (areas of normalized peaks, counts × keV)								
							Fe (Kβ1,2)	Mg (Kα1,2)	Zn (Kα1,2)	Mn (Kα1,2)	Ni (Kα1,2)	Cr (Kα1,2)	Sr (Kα1,2)	Ti (Kα1,2)	K (Kα1,2)
5	Chuncheon, South Korea	light grayish white	L* 42.75 a* −1.86 b* −3.34	622	459	1.09	1.39×10^4	4.75×10^3	3.86×10^3	2.24×10^4	–	1.28×10^3	7.09×10^3	–	–
7	Xiaomeiling, Kiyang county, Jiangsu province, China	light greenish white	L* 73.72 a* −4.77 b* 4.39	640	532	1.64	1.16×10^4	4.69×10^3	6.11×10^3	5.26×10^3	–	1.36×10^3	7.85×10^4	1.62×10^3	5.04×10^3
2	Liaoming Province, Xiuyan county, China	light greenish yellow	L* 57.12 a* −3.62 b* 0.85	624	500	0.61	2.14×10^4	6.38×10^3	1.36×10^4	7.92×10^3	–	2.86×10^3	–	2.30×10^3	2.55×10^3
9	Tao river Valley, Lintao, Gansu province, China	light green	L* 55.60 a* −10.27 b* 9.10	621	521	1.37	2.62×10^4	5.62×10^3	9.87×10^3	2.40×10^3	–	1.28×10^3	–	–	4.28×10^3
11	Tao river Valley, Lintao, Gansu province, China	greenish yellow	L* 29.55 a* −4.66 b* 2.26	629	499	0.64	1.59×10^4	5.05×10^3	5.17×10^3	6.46×10^3	–	1.32×10^3	–	2.90×10^3	6.80×10^2
3	Hualien, near Fentien, Taiwan	olive green	L* 29.40 a* −2.99 b* −0.39	630	528	13.23	2.02×10^5	3.41×10^3	6.79×10^3	2.13×10^4	4.61×10^4	1.59×10^4	–	–	–
10	Tao river Valley, Lintao, Gansu province, China	brownish green	L* 15.29 a* −5.06 b* 4.29	620	513	3.06	7.37×10^4	4.79×10^3	6.51×10^3	1.23×10^4	–	1.28×10^3	–	–	4.62×10^2

Table 2 Early Chinese jades from the collection of the Art Institute of Chicago, arranged in descending order from lightest to darkest in color

Object description, AIC accession no.	Attributed date	Color	Apparent composition (Raman) (Fe/Fe+Mg) (% p.f.u.)
Ring (huan), 1950.540	Neolithic period, probably Liangzhu culture, third millennium BCE	ivory white	0.37
Collared disc, 1950.240	Late Neolithic / Shang dynasty, second millenium BCE	very pale green, mottled	0.87
Blade (zhang), 1950.318	Late Neolithic / early Shang dynasty, second millenium BCE	dark green, almost black	29.73

A Rontec (Bruker, Berlin, Germany) ArtTAX noninvasive portable microfocus XRF system with an Mo excitation tube was employed, with a voltage of 50 kV, a current of 800 μA and He flushing to enhance the detection of low-Z elements. A live time of 200 seconds was used for all geological nephrite specimens analyzed, so that after curve fitting and normalization for the Ca peak, areas of all peaks could be calculated and the relative abundance of each element could be comparatively evaluated in a semiquantitative way.

Visible spectrophotometry was performed with a SpectroEye spectrophotometer (GretagMacbeth, New Windsor, NY, USA) over the range 380 nm to 730 nm with 10 nm resolution; 45°/0° geometry and a gas-filled tungsten type A illumination source were used. Data are presented for illuminant C and a 2° observer.

Most Raman microscopy (RM) data were acquired using a Jobin Yvon Horiba (Edison, NJ, USA) Labram 300 confocal Raman microscope , equipped with three excitation laser lines (λ_0=532 nm; 632.8 nm and 785.7 nm). Power at the surface of each jade was kept low in order to avoid thermal damage (measured at 0.94 mW and 3 mW for 532 nm excitation at two different neutral density filters settings, with an 100× microscope objective). A battery-powered Raman spectrometer (model Inspector Raman, with a 70 mW diode laser excitation of λ_0=785 nm, and 10 cm^{-1} resolution, manufactured by DeltaNu (Laramie, WY, USA, see http://www.deltanu.com) was also used.

X-ray diffraction (XRD) of the nephrite specimens and Chinese jades was carried out on a Scintag Diffractometer (Scintag Inc., XDS 2000, Cupertino, CA, USA) with Cu Kα radiation at 40 kV and 20 mA. Each spectrum was collected from 8° to 70° 2θ with a step size of 0.1° 2θ and a count time of 3 s. Surfaces used for diffraction were either polished or naturally flat. Silicon powder was dispersed on each surface as an in situ calibration standard. Since the strongest Si peak (28.466° 2θ) overlaps with nephrite peaks of interest, the second-strongest Si peak at 47.344° 2θ was used for calibration.

Results and discussion

Phase identification

In addition to XRD, RM is emerging as a valuable analytical technique for in situ phase identification of Chinese jades. Since different laser lines have been reported for the characterization of nephrite (tremolite and actinolite) and other amphibole minerals [9, 15, 18–20], the spectral quality of Raman data collected at three different excitation wavelengths on a late Neolithic/early Shang blade (*Zhang*) were compared to determine optimized collection conditions. In situ XRD analysis shows that this jade is composed of ferroactinolite ($Ca_2Fe_5Si_8O_{22}(OH)_2$; JCPDS 23-0118) with minor impu-

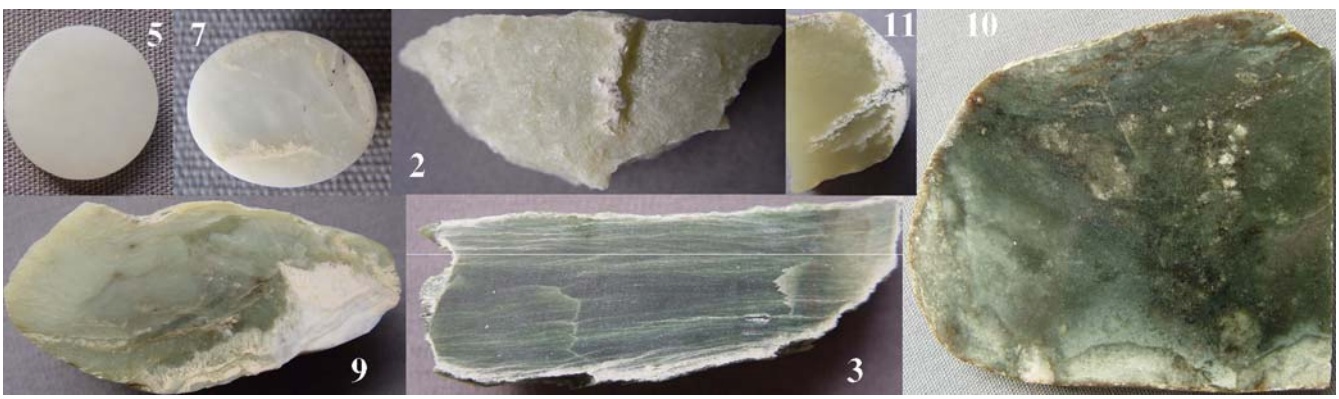

Fig. 1 Modern reference geological samples of nephrite from China and neighboring regions

Fig. 2 Jade objects from the collection of the Art Institute of Chicago (1950.540; 1950.240; 1950.318; Bequest of Mrs Edward—Louise B.—Sonnenschein)

rities of chlorite (clinochlore; JCPDS 10-0183), and ESEM/EDX shows it contains approximately 8% Mg, 5% Fe, 0.8% Al and 0.3% Mn. Although the *Zhang* blade shows one of the highest fluorescence backgrounds of all jades examined, it was possible to detect diagnostic spectral features with all three laser excitations (Fig. 3).

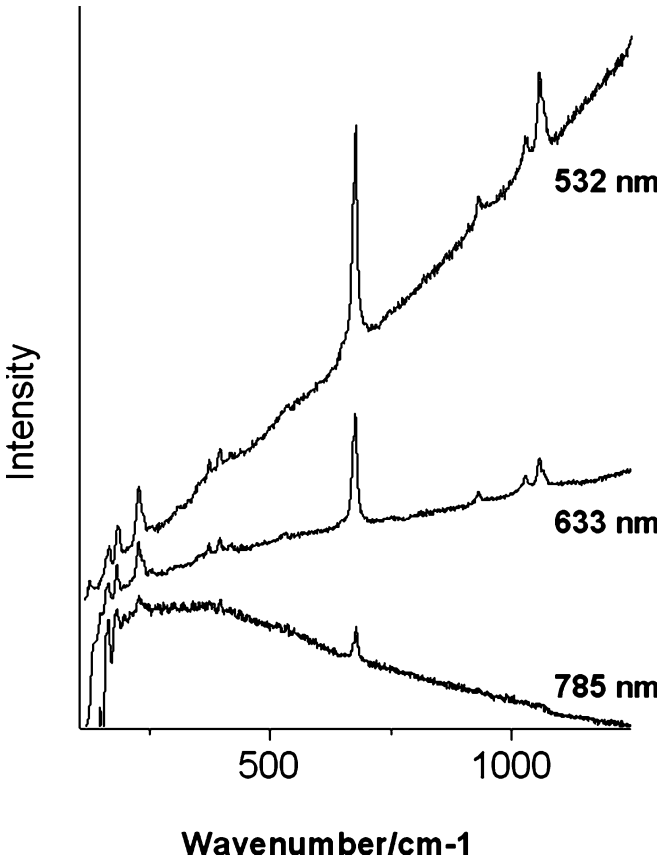

Fig. 3 Spectra obtained from a *Zhang* blade (nephrite, Late Neolithic/early Shang dynasty, second millennium BCE) with several excitation lines (no multipoint baseline correction was applied to the data)

However, based on further tests on other nephrite specimens, the 532 nm laser was selected as the most effective and versatile for successful collection of detailed spectra on jades of various colors. Fluorescence was not completely avoided, even using a 785 nm laser such as the one integrated into the portable RM. However, 30-s collection times allowed the acquisition of high-quality spectra on most geological specimens with the portable instrument. An exception was sample 7, which proved too fluorescent. All of the diagnostic bands for nephrite are recorded (Fig. 4), thus demonstrating the successful application of a field-portable Raman spectrometer to Chinese jades for the first time. Unfortunately, the lower resolutions of such instruments limit the resolution of the bands in the region 200–300 cm^{-1} (the external lattice mode region, with characteristic vibrations of O–H–O groups) and 300–450 cm^{-1} (dominated by bands attributed to Si–O–Si and O–Si–O bending modes and metal–oxygen bands), vibrations that are characteristic of nephrite (tremolite–actinolite) and allow their clear distinction from other amphibole minerals. Moreover, analysis with incident excitation light of 785 nm precludes examination of the spectral region centered at 3650 cm^{-1}, which offers some useful features. The availability of a benchtop spectrometer is always advantageous, as it offers higher spectral resolution and more flexibility in the selection of multiple excitation wavelengths; however, portable RM carries an evident advantage for the in situ examination of excavated jades at archaeological sites, allowing fast and unambiguous discrimination of nephrite jades from other stone artifacts.

XRD results for the geological specimens demonstrate a shift from tremolite (JCPDS 44-1402) in samples 5 and 7 to actinolite (JCPDS 41-1366) in samples 11 and 10 (Fig. 5). Although peak intensities do not correspond well to calculated values, peak positions show relatively good agreement across the monoclinic spectrum. The lack of agreement in relative intensity is not surprising, as preferred orientation in bulk specimens is likely to confound peak-matching programs. In addition to the

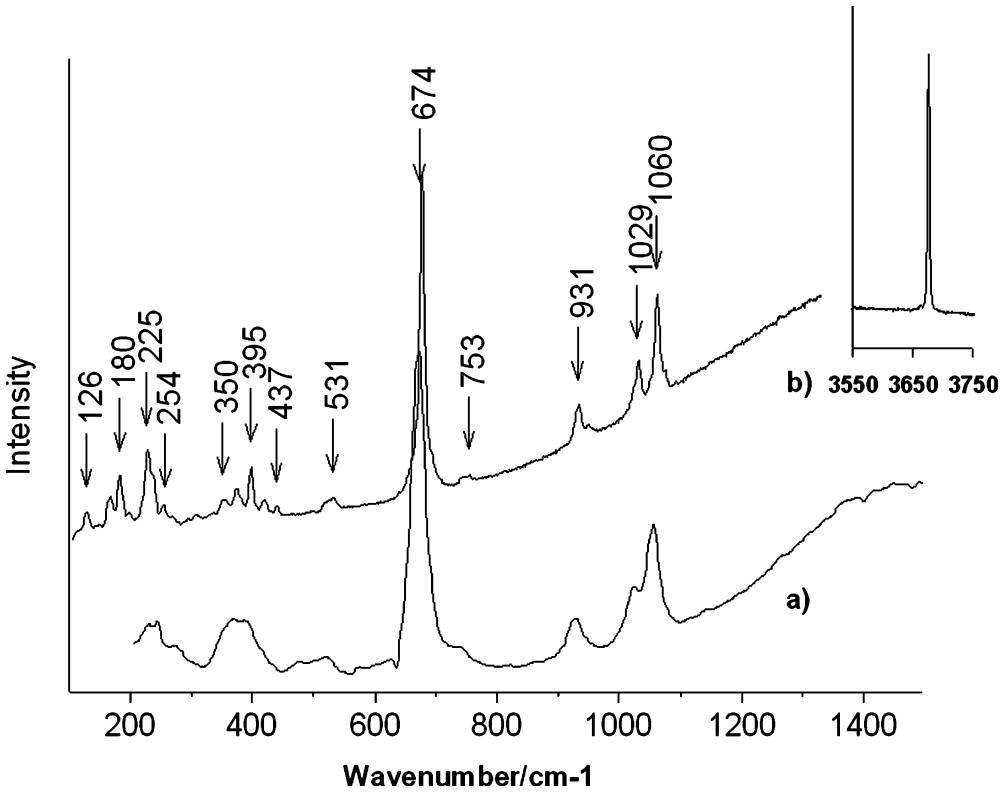

Fig. 4 Comparison of spectra recorded on nephrite geological reference sample 11 with the portable (**a**; λ_0=785 nm) and bench-top (**b**; λ_0=532 nm) micro-Raman spectrophotometer (spectra have been normalized with respect to the sym Si–O–Si stretching band centered at 673 cm^{-1} to facilitate comparison). The *inset* shows details of the spectral features in the O–H stretching region, detectable only with 532 nm excitation

tremolite or actinolite spectra, there are a few unidentified trace peaks. In the actinolite samples, peaks shift to lower angles by as much as 0.2° 2θ. This is especially pronounced in samples containing the highest Fe fraction (sample 10). This is demonstrated in the enlarged view of the 18 to 28° 2θ region in Fig. 6. Both of these observations are consistent with the substitution of the larger Fe^{2+} cation on Mg^{2+} sites, which increases the lattice parameter and hence decreases the diffraction angle. Evans and Yang verified this in a wide range of actinolite/tremolite single

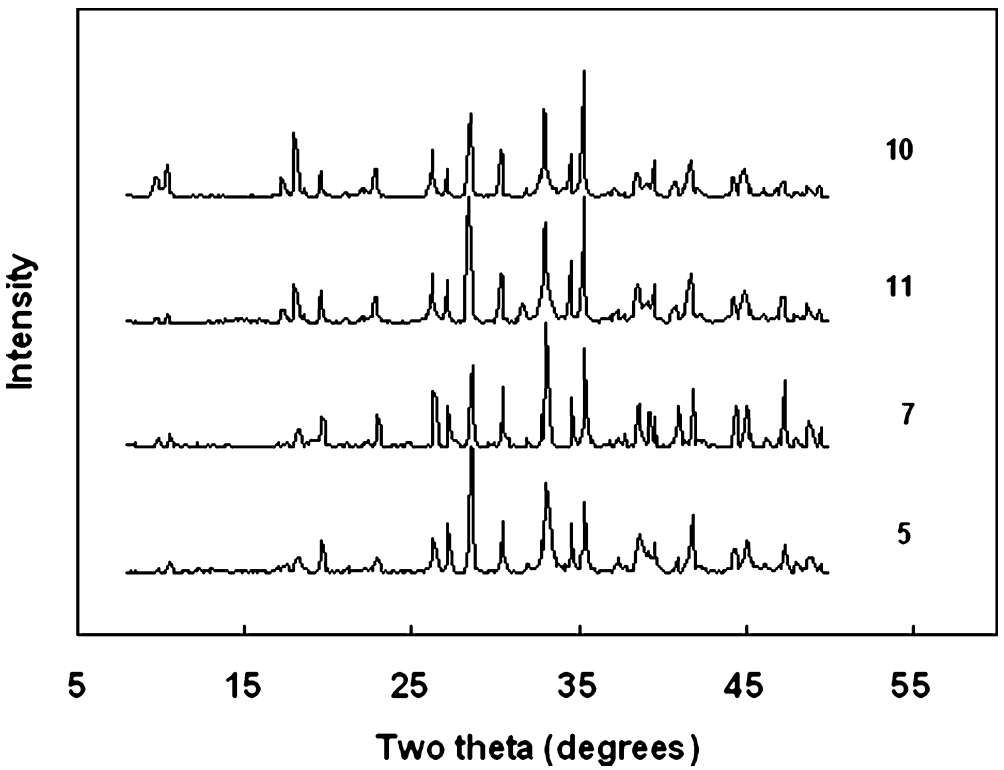

Fig. 5 X-ray diffraction spectra for samples 5 and 7, tremolite, and samples 11 and 10, actinolite

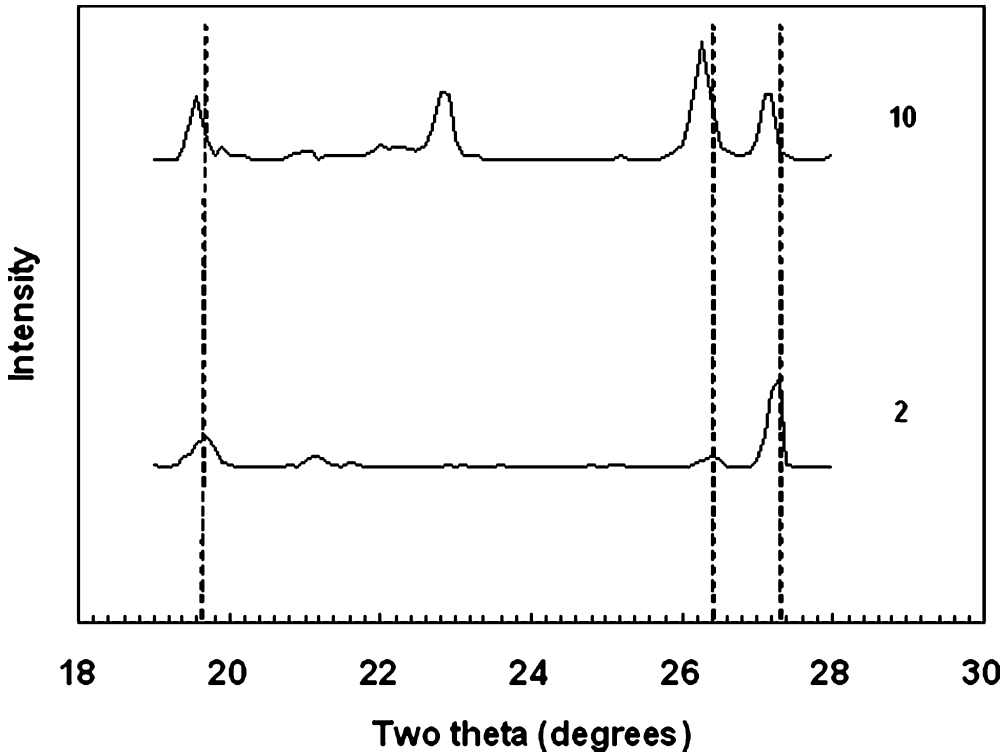

Fig. 6 Enlarged view of X-ray diffraction of actinolite samples 2 and 10, shown to demonstrate the peak shifts with increasing Fe content

crystals [21]. Although the higher Fe content and light-to-dark green color correlate with the actinolite spectra, selective XRD peak analysis over longer counting times would be required to quantitatively assess peak shift with color.

Elemental composition and color

As shown in Table 1, XRF of the geological reference specimens confirmed that the compositional variabilities of these nephrites fell within a narrow range for most. Exceptions are sample 3 from Taiwan, showing significantly higher contents of Fe, Ni, Cr, and Mn with respect to the other Chinese nephrites, and two samples from Xiaomeling, Jiangsu province, showing unusually high contents of Sr, thus easily separating them from the rest of the group (sample 7 is shown as representative example in Table 1). In agreement with data on New Zealand nephrite [10], data collected for this study indicate that cationic content does not easily correlate with the perceived color of the jades.

For example, if one follows the variation in color with Fe content, CIELAB coordinates calculated for the visible spectra recorded on differently colored jades in order to acquire numerical information on color [22–24] showed sample 10 (brownish green) to have the lowest L* value, even though its Fe content is approximately three times lower than sample 3 (olive green) (Table 1). Almost identically low values of L* were measured for samples 11 (yellow-green) and 3 (olive green), even though the latter has approximately thirteen times the Fe content of the former. High variability was observed in particular for the low-iron nephrites, whose colors vary from white to yellow-green in a nonmonotonic fashion with increasing Fe content. For example, samples 5 (white) and 11 (yellow green) have comparable total Fe contents, with the white nephrite showing a higher Fe/Fe+ Mg (% p.f.u.) ratio. Thus, although previous research has suggested that increasing Fe content in nephrite is correlated with a darkening of the color [1], a simple linear correlation does not apply.

Visible reflectance spectra recorded on the geological specimens are consistent with extensive discussions in the literature on amphibole minerals [25, 26]. Two dominant processes are responsible for the spectral features observed in the electronic spectra of nephrite: metal to ligand charge transfer (MLCT: $Fe^{2+}\rightarrow O$) involving Fe^{2+} in M1, M2, M3 and M4 sites and Fe^{3+} and Cr^{3+} in M2, M1 and M3 sites; and homonuclear ($Fe^{2+}\rightarrow Fe^{3+}$) or heteronuclear ($Fe^{2+}\rightarrow Ti^{4+}$) intervalence charge transfer (IVCT). Most samples analyzed for this study clearly showed the tail of the MLCT $Fe^{2+}\rightarrow O$ band, a band that has its absorption maximum in the higher energy UV region (Fig. 7a). All of the samples also exhibited a decrease in the reflectance factor at around 700 nm, related to Fe^{3+} spectral features. Only sample 3 showed weak absorption bands at 630, 658 and 691 nm, due to the presence of Cr^{3+}(Fig. 7b), detected by XRF in relatively high abundance solely for this sample. Sample 3 also showed a small absorption at 420 nm due to a Fe^{3+} crystal field (CF) transition, with other weak absorptions at 400–600 nm associated with spin-forbidden bands of Fe^{2+}. With the exception of sample 5, which is white in color, and has a maximum

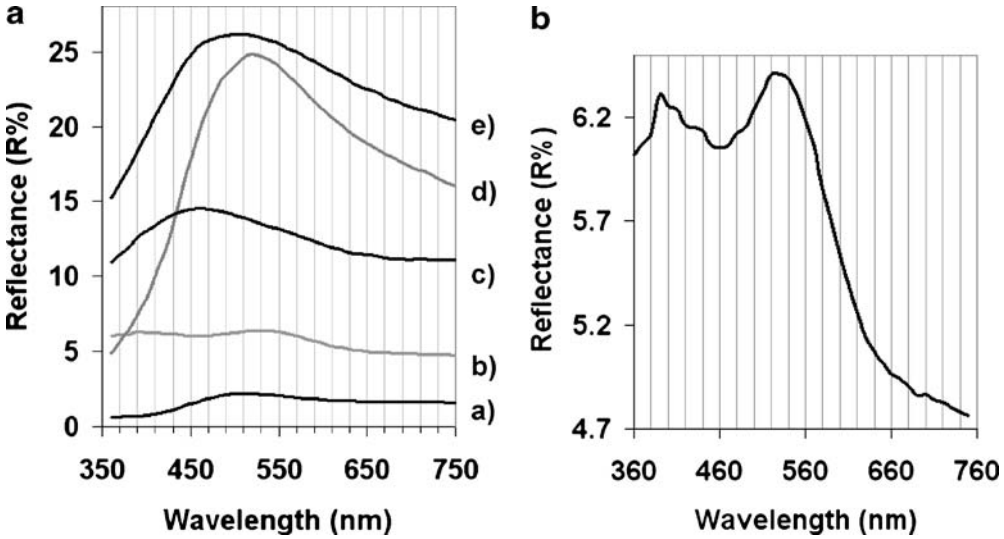

Fig. 7 a,b **a** Visible reflectance spectra of geological nephrite samples: *a* 10; *b* 3; *c* 5; *d* 9; *e* 2. **b** Detail of the visible reflectance spectrum of nephrite sample 3, showing characteristic spectral features linked to the presence of Fe^{2+}, Fe^{3+} and Cr^{3+} ions

reflectance factor (λ_{max}) at 459 nm, all of the other samples owe their green color to a λ_{max} in the green portion of the visible spectrum between 500 and 530 nm.

Previous research has suggested that relatively high chromium content in nephrite can be detected by a "strong intensity in the Raman spectra in the 6000 cm^{-1} range" ([8], p. 34); however, this study did not confirm such a linear influence of the presence of Cr in the high wavenumber region of the Raman spectra. In fact, with the exception of sample 3, characterized by significant Cr content, all other geological reference samples examined had only trace amounts of Cr (reported in [14] at 0.05–0.07%). Nevertheless, Raman spectra for samples 10 and 7 also showed an increasing slope in the baseline at wavenumbers higher than 4000 cm^{-1}. This spectral feature seems rather to correlate with higher reflectance in the red region of the visible portion of the spectrum. Those samples (2, 5, 9, 11) that, on the contrary, show an absorption in such region have flat baselines at wavenumbers higher than 4000 cm^{-1} (Figs. 7 and 8). These findings underscore the need for a more critical, less simplified approach towards the assessment of the complex interrelation between color, cation composition, and broad features in the Raman spectra.

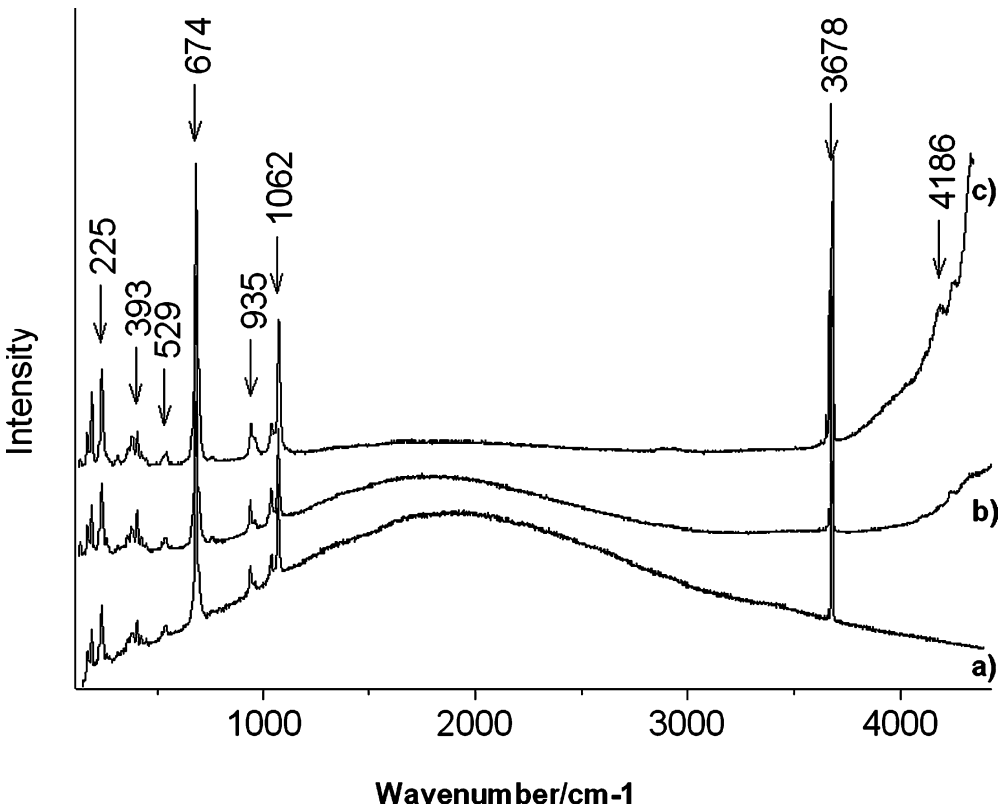

Fig. 8 Micro-Raman spectra of nephrite samples 3 (**c**) and 10 (**b**) showing a sloping, increasing baseline feature at wavenumbers higher than 4000 cm^{-1} and sample 9 (**a**), showing a lack thereof (λ_0=532 nm)

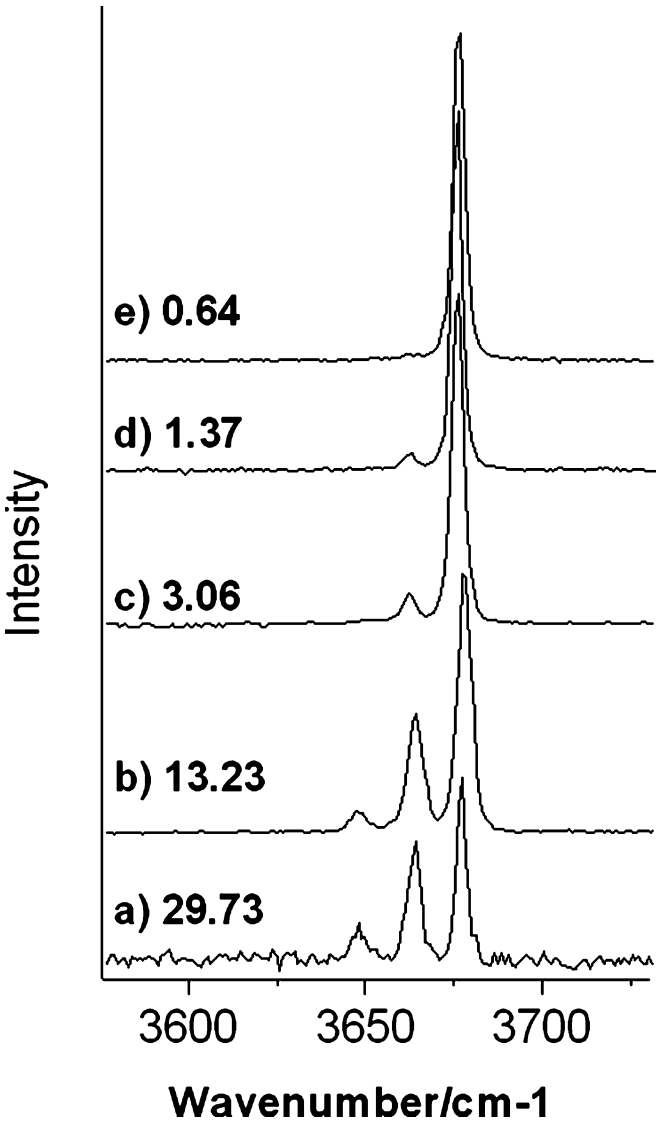

Fig. 9 Micro Raman spectra of (**a**) blackish *Zhang* blade, (**b**) olive green nephrite, sample 3, (**c**) brownish green nephrite, sample 10, (**d**) light green nephrite, sample 9, (**e**) greenish yellow nephrite, sample 11 (λ_0=532 nm; after multipoint baseline subtraction). For ease of reference, each respective Fe/Fe+Mg (% p.f.u.) ratio derived from the normalized intensity of the Raman band in this region is given

Structural implications for the determination of geological origin

The crystal structure of nephrite consists of a double-chain silicate with brucite-like strips sandwiched between opposed silicate chains with linking cations of nearly octahedral coordination [15]. A recent study by RM [15] demonstrates that analysis of the fine structure associated with the O–H stretching Raman bands of nephrite allows the cationic substitution of Fe (or, more precisely, Fe+Mn) to be determined for Mg in M1 and M3 sites. This allows a reasonable approximation of the Fe content in nephrite to be made, which, in turn, can be correlated to the geological origin of the material: from nephrite deposits associated with magnesian marbles or with serpentinized ultramafic rocks [1]. Fe/Fe+Mg ratios (% p.f.u.: X_R% in the following) of between 0.4 and 7.4 can be ascribed to magnesian marbles (dominant in mainland China), and values >8.1 to serpentinized ultramafic rocks (more common in other regions worldwide). In the present study, only samples with X_R% >10 showed significant splitting of the O–H stretching band (centered at 3675 cm^{-1} and the only one observed when Mg is the sole occupant of the M1 and M3 sites), with a medium peak at 3664 cm^{-1} (indicative of MgMgFe or MgFeMg occupancy) and emergence of the peak at 3645 cm^{-1}, indicative of FeFeMg or FeMgFe substitution (observed as a weak but well-defined peak only for sample 3 and for the dark-colored *Zhang* blade). At X_R% >3, one clearly observes a small peak at 3662 cm^{-1}, while at X_R%~1 only a very weak peak at this wavenumber is discernable (Fig. 9).

Heat treatment of nephrite

RM also proved invaluable for the noninvasive detection of instances of heat treatment in nephrite, a phenomenon previously studied with XRD and Fourier transform infrared spectroscopy (FTIR) on samples removed from the jades [17]. Artificial jade treatment is of great interest to archaeologists and art historians studying Chinese jades, because its detection and identification allows a deeper understanding of the culture that produced and used such objects. With regards to heating, two principal theories have been proposed: some jades may have been heat-treated to soften the stones prior to working them; alternatively, jades may have been subjected to heat during ritual ceremonies. Additionally, detection of heat treatment is of importance because forgers are thought to treat modern jade objects with heat in order to simulate the whitened, altered appearance of ancient jades.

The dehydration process of tremolite/actinolite as well as the colors observed following heating have been previously described by Douglas [17]. The color changes exhibited by the low-iron nephrite pebble used in this study, from translucent grayish yellow green to opaque white with increasing temperature (Fig. 10), are connected to a solid-state reaction where diopside and cristobalite pseudomorphs of tremolite crystals are generated following the reaction:

$$\underset{\text{nephrite(tremolite)}}{Ca_2Mg_5Si_8O_{22}(OH)_2} \xrightarrow{\Delta} \underset{\text{pyroxene(diopside)}}{2CaSiO_3 \cdot 5MgSiO_3} + \underset{\text{cristobalite}}{SiO_2} + \underset{\text{water}}{H_2O}$$

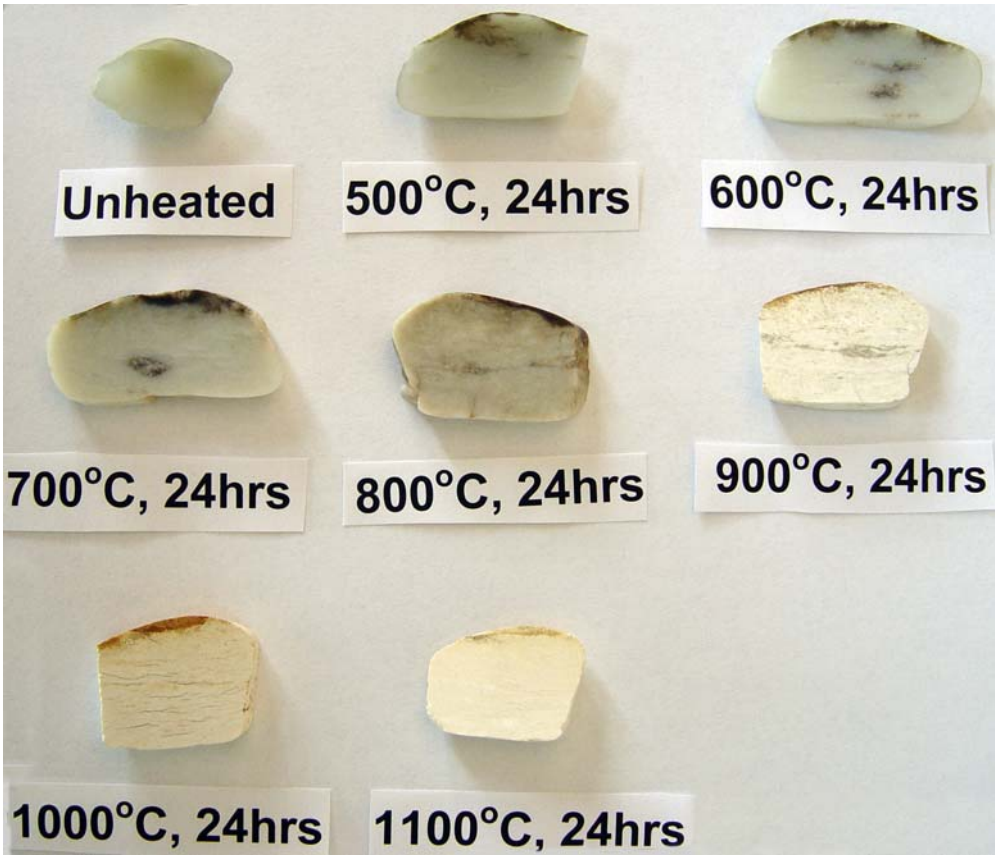

Fig. 10 Slices of a low-iron nephrite pebble from Hetian (Khotan), Xinjiang province, heated individually to increasing temperatures up to 1100 °C (the largest slice measured approximately 3 cm)

Some darkening was observed at the edges of the nephrite specimens heated from 500 °C to 800 °C, successively turning from a reddish brown color at 900 °C to an orange-red color at 1100 °C. In the corresponding area of the unheated nephrite sample, the material has a slight greenish color, possibly representing a relatively Fe-rich area.

Because of its high spatial resolution and ability to detect mineral oxides, RM allowed the characterization of the origin of the blackish and reddish color that develops at the uppermost surfaces of the samples and whose nature was previously only hypothesized. As illustrated in Fig. 11, the present analysis shows that finely dispersed carbonaceous particles, together with localized accumulation of Fe oxidation products (hematite, magnetite and possibly maghemite or other Fe oxides characterized by a band at 700 cm^{-1}) are responsible for the brownish color of the slices heated between 600 °C and 800 °C [27]. Only hematite and magnetite are detected at 900 °C and at 1000 °C, while at 1100 °C the diagnostic peaks for hematite and diopside are detected together, suggesting that these two minerals are intimately mixed.

With respect to changes affecting the bulk of the heated samples, ten to fifteen areas were probed on each slice representative of a discrete temperature step, and the spectra collected confirmed that no structural or chemical change is detectable for temperatures up to 900 °C: in fact, only the characteristic bands of nephrite are evident (with bands at 129 m, 162 m, 224 m, 251 vw, 266 vw, 302 vw, 351 vw, 369 w, 393 m, 416 w, 437 vw, 526 w, 673 vvs, 930 m, 948 w, sh, 1029 m, 1060 s, 3662 vw, 3676 vs cm^{-1}). Starting at 900 °C, the bands of diopside (198 w, 233 w, 329 m,395 m, 560 vw, 668 s, 1013 vs cm^{-1}) are detected, sometimes together with those of nephrite, as illustrated in Fig. 12, clearly indicating that structural and chemical change is either in its inception or in full progress or completed at this temperature, depending on the specific area probed. In some areas of the specimen heated up to 900 °C, nephrite is the most predominant phase, in other areas it is diopside. In the O–H stretching region, the band at 3675 cm^{-1} decreases in intensity and broadens as a result of oxidation of Fe ions present in the lattice, while the weak band at 3661 cm^{-1} disappears (disappearing at 800 °C). Finally, at 1000 °C and 1100 °C no spectral feature is detected in the O–H stretching region, confirming that the only phase remaining is diopside.

The RM study of heating described here corroborates previously published results obtained with FTIR on samples removed from the same specimens and analyzed in a diamond microcompression cell [17]. However, RM benefits from higher spatial resolution (over one order of magnitude lower, as microsampling affects areas of the order of millimeters) and, being noninvasive, allows thorough mapping of the entirety of the objects examined. The detection of isolated crystals of diopside in the uppermost areas of the nephrite pebble heated as low as

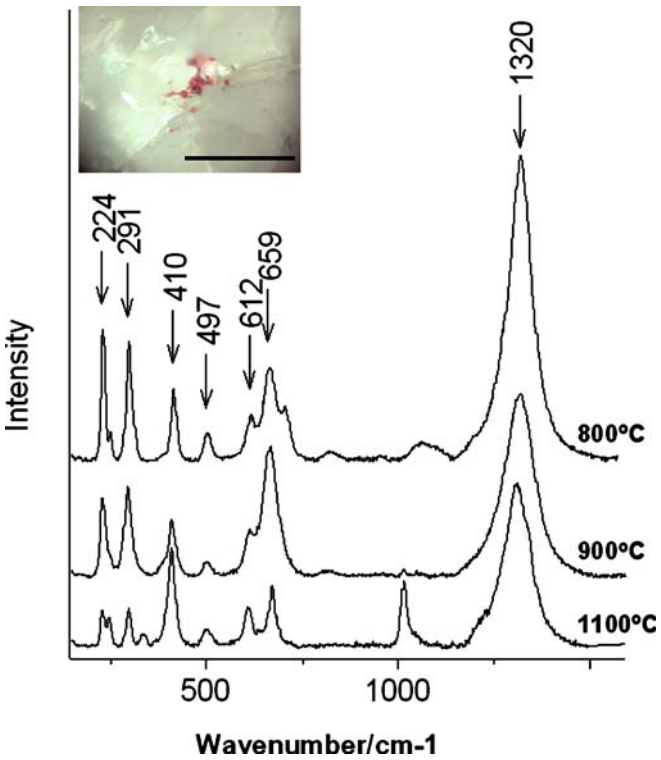

Fig. 11 Micro-Raman spectra of the oxidation products of Fe compounds conferring a characteristic reddish brown color to the uppermost surface of the heated jades (λ_0=532 nm; after multipoint baseline subtraction). At 1100 °C only diopside and hematite are evident, at 900 °C hematite and magnetite, at 800 °C hematite, magnetite and maghemite. In the *inset*, a microphotograph acquired through the integrated microscope of the Raman spectrometer shows the particles of iron oxide interdispersed in the nephrite/diopside matrix in the heated samples (the bar measures 250 μm)

600 °C (an inhomogeneity in the nephrite) demonstrates that caution should be exercised when analysis has to rely on the removal of only one small sample from a determinate area.

Conclusions

This study presents an innovative, totally noninvasive approach to the study of Chinese jades, using complementary analytical methods to not only identify nephrite but also to characterize important parameters related to color, geological origin and natural or human-induced alterations. Visible spectrophotometry provided accurate measurements of color, although the complex electronic spectra obtained for the different geological samples reflect the extreme variability in the color and shade of nephrite, and their detailed interpretation will require further study. The techniques of RM, XRD, and XRF are rapid and effective means to provide in situ jade characterization, and together they provide data on mineralogical identification, elemental composition, and crystallographic structure. In particular, RM has great potential as it allows selective study of the surface structure of jade at the microscopic level in order to identify features such as heating, accretions, color shading, and texture. Although resolution is limited, portable RM is particularly useful for field applications, allowing for rapid discrimination of nephrite from jadeite (not documented in the context of Chinese jade artifacts before the eighteenth century) and other jade-like stone materials such as quartz, calcite, serpentine, chlorite, and talc. The use of RM to determine Fe/Fe+Mg ratios (% p.f.u.) in jades has proven useful as a method of classifying artifacts and gaining insights into their geological origins.

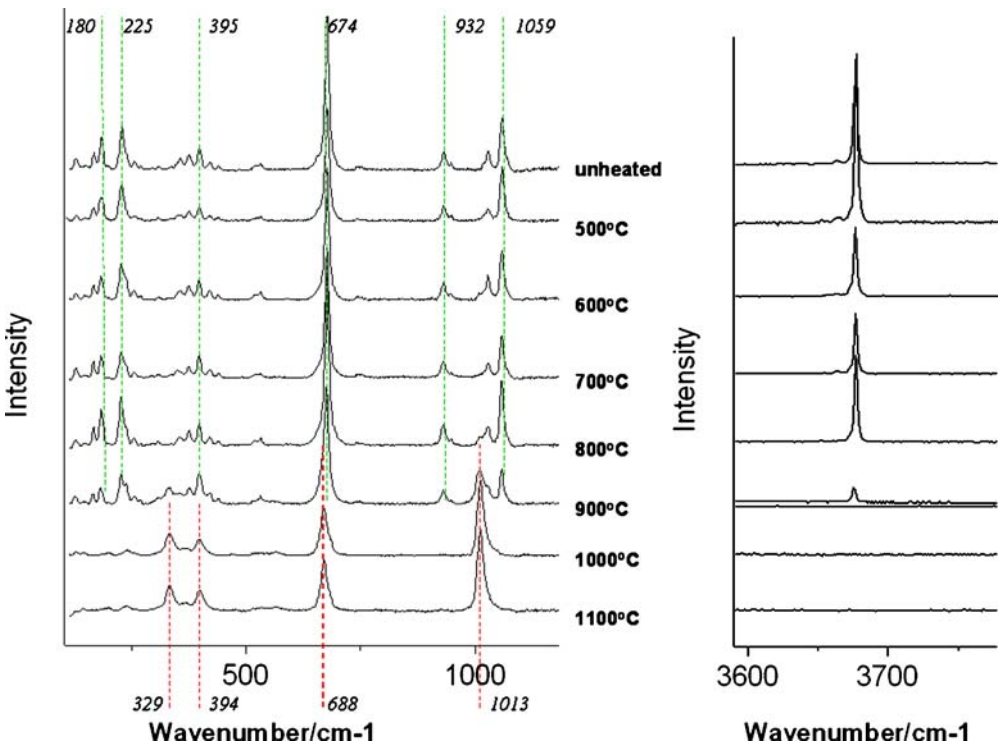

Fig. 12 Raman spectra excited with 532 nm laser on the slices of low-iron nephrite pebble heated in discrete steps from 0 to 1100 °C, illustrating chemical and structural changes associated with heating. At *top*, characteristic Raman bands for nephrite are marked, at *bottom*, the characteristic bands for diopside. At *right*, the O–H stretching region is shown, with two curves for the sample heated to 900 °C to illustrate the presence of either nephrite or diopside in the different areas probed. (All spectra shown after multipoint baseline subtraction)

The accumulation of a database of Fe/Fe+Mg (% p.f.u.) ratios from scientifically excavated archaeological objects and well-documented museum objects will prove invaluable for the ultimate provenancing of undocumented Chinese jades.

Acknowledgements Conservation science research at the Art Institute of Chicago is made possible by a generous grant from the A. W. Mellon Foundation. The Community Associates of the Art Institute are thanked for their support of the microfocus XRF. Elinor Pearlstein and Jay Xu, curators of Asian Art at the Art Institute of Chicago, are also thanked. The assistance of Susie James, Alyson Whitney, Jerry Carsello and Benjamin Meyers for data collection at Northwestern is gratefully acknowledged. X-ray facilities at NU are supported by the MRSEC program of the National Science Foundation (DMR-0076097) of the Materials Research Center of Northwestern University. Wen Guang, Feng Min, Tan Li-ping and Joseph Hotung are thanked for providing reference nephrite samples.

References

1. Wen G, Jing Z (1996) Acta Geol Taiwan 32:55–83
2. Douglas JG (2005) A review on some recent research on early Chinese jades. In: Scientific examination of art: modern techniques in conservation and analysis, from the Arthur M. Sackler Colloquia of the National Academy of Sciences. The National Academies Press, Washington, DC, pp 206–214
3. Wen G (1997) Colloq Art Archaeol Asia 18:105–122
4. Wen G (1998) In: Tang C (ed) East Asian jades: symbol of excellence, vol. 2. Chinese University of Hong Kong, Hong Kong, pp 217–221
5. Wen G, Jing Z (1992) Geoarchaeology 7:251–255
6. So J, Douglas JG (1998) Understanding and identifying jades from the Hongshan Culture. In: East Asian jades: symbol of excellence, vol. 1. The Chinese University of Hong Kong, Hong Kong, pp 148–163
7. Casadio F, Xu J, Pearlstein, Faber KT, Knowles A, Jing Z (2006) A stone kneeling figure in the Art Institute of Chicago: new evidence from scientific investigations and archaeological finds in China. In: Douglas JG, Jett P, Winter J (eds) Scientific Research on the Sculptural Arts of Asia, Proceedings of the Third Forbes Symposium at the Freer Gallery of Art. Archetype Publ., London (in association with the Freer Gallery of Art, Smithsonian Institution, Washington, DC) (in press)
8. Xu JN, Huang E, Chen CH, Tan LP, Yu BS (1996) Acta Geol Taiwan (Special Issue on the Mineralogical Study of Archaic Jades) 32:11–42
9. Shurvell HF, Rintoul L, Fredericks PM (2001) Int J Vibr Spec 5 (5):4 (see http://www.ijvs.com)
10. Wilkins CJ, Tennant CW, Williamson BE, McCammon CA (2003) Am Mineral 88:1336–1344
11. Gendron F, Smith DC, Gendron-Badou A (2002) J Archaeol Sci 29:837–851
12. Smith DC, Gendron F (1997) J Raman Spectrosc 28: 731–738
13. Douglas JG (1996) Acta Geol Taiwan (Special Issue on the Mineralogical Study of Archaic Jades) 32:43–54
14. Douglas JG (2003) Exploring issues of geological source for jade worked by ancient Chinese cultures with the aid of X-ray fluorescence spectroscopy. In: Jett P, Douglas JG, McCarthy B, Winter J (eds) Scientific Research in the Field of Asian Art, Proceedings of the First Forbes Symposium at the Freer Gallery of Art. Archetype Publ., London (in association with the Freer Gallery of Art, Smithsonian Institution, Washington, DC), pp 192–199
15. Chen TH, Calligaro T, Pagès-Camagna S, Menu M (2004) Appl Phys A 79:177–180
16. Middleton A, Ambers J (2006) Case study: Analysis of nephrite jade using Raman microscopy and X-ray fluorescence spectroscopy. In: Edwards HGM, Chalmers JM (eds) Raman spectroscopy in archaeology and art history. Royal Society of Chemistry Analytical Spectroscopy Monographs, Cambridge, UK, 23:403–411
17. Douglas JG (2001) The effect of heat on nephrite and detection of heated Chinese jades by X-ray diffraction (XRD) and Fourier-transform infrared spectroscopy (FTIR). In: Proc Conf Archaic Jades Across the Taiwan Straits. Taipei, Taiwan, pp 543–554
18. Blaha JJ, Rosasco GJ (1978) Anal Chem 50(7):892–896
19. Lewis IR, Chaffin NC, Gunter ME, Griffiths PR (1996) Spectrochim Acta Part A 52:315–328
20. Rinaudo C, Belluso E, Gastaldi D (2004) Miner Mag 68 (3): 455–465
21. Evans BW, Yang H (1998) Am Mineral 83:458–475
22. Berns RS (2000) Billmeyer and Saltzman's principles of color technology, 3rd edn. Wiley, New York
23. International Commission on Illumination, Bureau Central de la CIE (1931) Proc 8th Session. Cambridge, England, pp 19–29
24. CIE (1986) Colorimetry, 2nd edn (No. 15.2). Commission Internationale de L'Éclairage, Vienna, Austria
25. Karr C Jr (ed) (1975) Infrared and Raman spectroscopy of lunar and terrestrial minerals. Academic, New York
26. Hunt GR, Salisbury JW, Lenhoff CJ (1973) Mod Geol 4:85-106
27. de Faria DLA, Silva SV, de Olivera MT (1997) J Raman Spectrosc 28:873–878